EXPERIMENTAL AND NUMERICAL EXAMINATION OF A HELICOPTER HOVERING IN GROUND EFFECT

Benjamin M. Kutz, Tobias Großmann, Manuel Keßler and Ewald Krämer
kutz@iag.uni-stuttgart.de, University of Stuttgart, IAG, Pfaffenwaldring 21, Stuttgart, 70569, Germany

Abstract

This study intends to collect experimental data of a helicopter hovering in ground effect and to prove the capability to compute the flow field around the measured helicopter rotor with the use of the flow solver FLOWer. Firstly the wake trajectory of a Hughes 300C helicopter hovering in ground effect was obtained by introducing fog in the rotor disk, while visualizing the blade tip vortices with a laser light sheet and a high speed camera. Secondly the isolated rotor of the Hughes 300C was modeled numerically and computed with the block-structured second order flow solver FLOWer from DLR, in order to provide a computational validation for full size rotors in ground effect hover. The blade dynamics were neglected and the rotor was trimmed to the experimental thrust. It was found that the flow solver is capable of simulating the flow around a full size helicopter rotor during hover in ground effect. The wake trajectories are convected downwards slightly faster than in the experiment. The radial wake path fits well with the experimental ones until high wake ages, where the numerically reproduced trajectory becomes unstable. The development in the thrust value was analyzed with a Fourier transformation. Disturbances of the ground can be detected especially at higher harmonics of the blade passing frequency. For comparison the rotor was also examined numerically out of ground effect. As expected the oscillations are lower than near to the ground. An analysis of the performance data lead to a benefit of 24% due to the ground effect.

NOMENCLATURE

η	efficiency factor [-]
Ψ	wake age [°]
g	gravitational acceleration [m/s^2]
h/R	height to ground ratio [-]
m	mass [kg]
M/b	shaft moment per blade [Nm]
P/b	power per blade [W]
T	thrust [N]
T/b	thrust per blade [N]
BPF	blade passing frequency
CFD	computational fluid dynamics
DLR	Deutsches Zentrum für Luft- und Raumfahrt e.V.
IAG	Institute of Aerodynamics and Gas Dynamics
IGE	in ground effect
OGE	out of ground effect
RANS	Reynolds averaged Navier Stokes

1 INTRODUCTION

The helicopter aerodynamics in ground effect are three dimensional and highly unsteady, therefore, they are not yet fully understood. The complex interactions between rotor, rotor-wake and ground provoke considerable effect on the helicopter. Knowledge of the flow field around the helicopter in proximity to ground is necessary, as it directly affects the handling qualities, performance data and flight safety of the occupants as well as ground personnel. Hence this flight state was subject of investigations for the last decades.
Previous studies were often carried out with model rotors out of ground effect flight (OGE)[1] or in ground effect (IGE) in hover[2] and forward flight[3],[4]. Experimental correlations like in Ref. 5 were extracted. As the time has advanced the numerical models and computational devices have become more sophisticated, so that the development has advanced from finite state modeling (Xin et al.[6]) over free vortex/ potential models (Bhattacharyya and Conlisk[7], D'Andrea[8]) to Euler- and Navier Stokes methods (Brown and Whitehouse[9], and Kalra et al.[10]).
In the present study an experimental and numerical examination of the wake of a full scale helicopter hovering in ground effect is presented. This study intends to obtain experimental data with correct Reynolds number, Mach number and scale, and to validate the Navier-Stokes computational fluid dynamics (CFD) code used at the Institute of Aerodynamics and Gas

Dynamics (IAG). In the past this validation was done with model data starting from a fixed wing in ground effect in Ref. 11, advancing to a helicopter rotor in hover IGE (see Ref. 12). Recently this was expanded towards forward flight in Ref. 13. Unsteady effects of the flow field IGE are also of interest as they directly influence e.g. the performance.

1.1 Experimental Setup

In the present study a Hughes 300C helicopter was used for the evaluation of the rotor wake. To visualize the blade vortices fog was introduced to the rotor disk, which was sucked in and convected downwards. A laser light sheet was spread with a $532nm$-laser and a high speed camera was used to obtain pictures for the evaluation.
Two test conditions were examined. Firstly, to obtain quantitative data of the wake propagation, the helicopter was hovering shortly above the ground. A second test was performed with the helicopter on ground with 75% thrust to achieve pictures which are good for a qualitative description of the wake development. In Fig. 1 a schematic picture of the setting is given. The hanger near the test-field had no effect on the rotor flow.

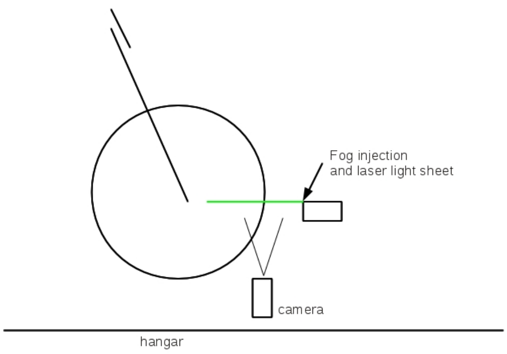

Fig. 1. Schematic setting of the experiment

1.1.1 Helicopter As discussed a Hughes 300C helicopter was used in the present study. Data characterizing the helicopter are given in Tab. 1. The helicopter was held in ground effect with skids close to the ground, which leads to a height to radius ratio of about $h/R = 0.7$ for this specific helicopter.

The thrust of the helicopter in hover can be derived from the mass and the efficiency factor. The efficiency factor describes the losses due to rotor-fuselage interactions. The value for this helicopter is not known,

Table 1. Helicopter Data

mass $[kg]$	782.5
skid height above ground $[m]$	$0.1 - 0.2$
height skids to rotor center $[m]$	2.67
number of rotor blades	3
rotor radius $[m]$	4.09
rotor frequency hover f $[Hz]$	7.85
rotor frequency 75%-test f_{75} $[Hz]$	6.17
chord $[m]$	0.173
blade twist $[rad/m]$	0.0549
airfoil	NACA 0015
blade mass $[kg]$	11.23

therefore, the value is set to $\eta = 1$. So the thrust is approximately

(1) $$T = \frac{m * g}{\eta} = 7.7kN.$$

1.1.2 Laser and fog system To visualize the wake of the helicopter rotor, the laser ”HB-Laser Lasersystem DPSS200 green” was used. This laser features a wavelength of $532nm$ and a power of $200mW$. A light section layer was generated by using a cylindrical lense with a focal length of $5mm$. To obtain enough fog to visualize the flow a ”Look Viper 2,6 Fog Machine” was used, employing a power of $2.6kW$.

1.1.3 High speed camera The high speed camera used was a ”Photron FASTCAM-Super 10K”. A Resolution of 512 x 480 Pixel was selected. In this examination 250 frames per second (fps) could be recorded, which results in a rotor motion of about $11.3°$ between two pictures. A higher frame rate could have been realized with a lower resolution, however, the resolution could not be reduced because of the phenomenon size to be measured.
A SOM Berthiot Cinor B c-mount objective was used. This possesses a focal length of $25mm$.

1.1.4 Ambient conditions The ambient conditions were measured and are tabulated in Tab. 2. The ambient wind can be neglected as the measurement took place at the lee side of a hangar. Even the ambient winds on the free surface were always below $2kt \sim 1m/s$. Free convection can be neglected compared to the speed of the downwash.

1.2 Numerical examination

The numerical examination of the experiment aims to validate the use of the state of the art CFD tool used at IAG and to obtain information of the governing flow

Table 2. Ambient conditions

airport height $[ft]$	1650
density height $[ft]$	1920
density $[kg/m^3]$	1.167
temperature $[°C]$	8
ambient winds below $[kt]$	2

physics IGE. The method and the setup will be described in the following.

1.2.1 Computational method The computations were performed with the block-structured Finite Volume second order Reynolds averaged Navier Stokes (RANS) CFD solver FLOWer[14] developed by DLR. The standard Wilcox k-ω model was used for turbulence modeling. The Chimera technique was chosen to handle blade grids and their relative motions. Via dissipation coefficients of order two and four the used central difference scheme is stabilized. This results in a second order accuracy in space. The procedure was introduced by Jameson, Schmidt and Turkel[15]. It was detected in previous studies (e.g. Ref. 13) that for ground effect calculations unsteady computations are mandatory. Therefore, a dual time stepping is used for temporal discretization (Jameson[16]). In this computation the aeroelastic deformation was neglected.
The rotor collective pitch was trimmed manually. As already mentioned η in Eq. 1 is not known, therefore, the rotor thrust was trimmed to the weight of the system ($\eta = 1.0$). That results in a trim target of the mean thrust per blade of $T/b = 2560N$.

1.2.2 Setup The hover setup is built up as a periodic one-third setup with about 13.8 million grid cells. For all IGE computations, a ground boundary condition which assures no-slip and zero mass flux is employed. At the blades and on the ground the resolution is high enough to simulate the boundary layer. To draw comparison an OGE calculation was conducted with the same mesh setup excluding the wall boundary condition at the ground.

1.2.3 Computational Resources All computations were performed on the Hermit Cray Cluster at the High Performance Supercomputing Center at Stuttgart (HLRS) on 192 cores. With a computational time step of $1°$ rotor azimuth, one revolution needs about eleven hours wall clock time. For the manual trim procedure several trim iterations were performed. Attention was also paid on the build up of a periodic flow field in each trim step. This resulted in about 26 revolutions of the rotor in total, which summed up to about twelve days wall clock time with the mentioned resources. In hover OGE nearly 7 revolutions were performed to achieve a converged flow field and to obtain a data base to be able to average the results.

2 RESULTS

2.1 Experiment

In the following section an overview of the experimental results is presented. First a qualitative discussion of the flow field is given, which was derived from the 75%-test, see Fig. 2. It can be stated that at the center of the vortex no fog is located. Secondly, the measurements of the wake paths are shown and quantized (Figs. 5 and 6).

Fig. 2. Blade tip vortices from the 75%-test (rotor disk in red)

2.1.1 Flow field It can be seen in Fig. 3 that the flow through the rotor features all characteristics of an impingement flow. The fog is sucked in, moves downwards and is then turned in outward direction. For the blade vortices it was found, that the vortex shows several characteristic movements during its way through the fluid. Following states were found from a series of pictures like Fig . 2:

- Fast vortex build up after a blade
- Slight inbound and upward movement
- Reversal of upward movement
- Inbound and downward movement under an angle of about $45°$ to the rotor disk

Due to the limited resolution and view angle of the camera, the vortex could not be tracked further downstream, moreover due to dilatation the visibility of the vortex became bad at higher wake ages than approximately $\Psi = 360°$. Despite this, a qualitative analysis can be drawn further according to Fig. 3.

- Vertical movement of the wake at about $1.5m$ above ground
- Outward movement in a radial direction as expected for hover IGE

Fig. 3. Helicopter hovering during tests

2.1.2 Wake path For the following examinations the helicopter was hovering slightly above the ground. The height was varying between $0.1m$ and $0.2m$ skid height above the ground. This range is due to the fact that the pilot can not hold the helicopter perfectly at only one position. As minor disturbances are introduced into the real system, the pilot has to react and try to hold the helicopter as still as possible in the hover condition. During the time of one measurement the helicopter can be assumed to be at one height. It can be supposed that on the mean value of the several measured vortices this behavior has no significant impact. Only a small shift in the h/R direction may be introduced by this in the path of one examined vortex. The coordinate system at the blade tip is

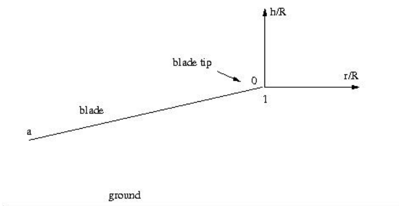

Fig. 4. Coordinate system

shown in Fig. 4. As the roll angle of the helicopter and the cone angle of the rotor almost cancel each other out in the measurement area, the angle between the blade and the coordinate system is small. The experimental results were, therefore, corrected with a rotation, as the computational result had no cone angle, to have a common basis for comparison. Nevertheless, the ground distance of the rotor is not constant during the whole revolution. Therefore, some aberrations between the experiment and the computations may occur. In previous examinations (Ref. 13) it was found out, that the ground effect has far more influence on the radial wake path than on the axial.

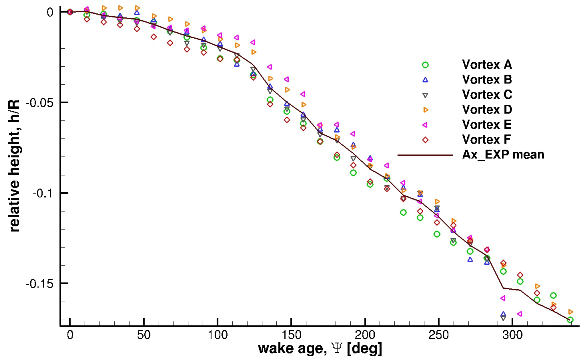

Fig. 5. Vertical movement of the measured wake

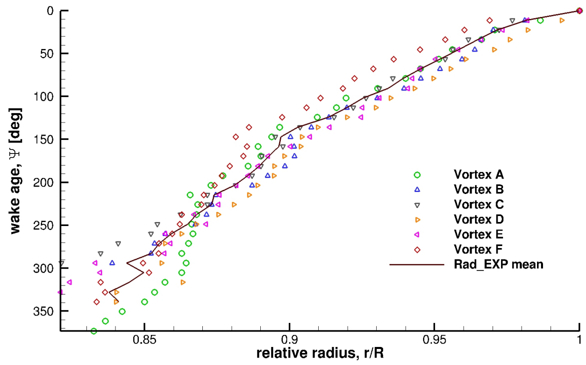

Fig. 6. Horizontal movement of the measured wake

In Figs. 5 and 6 the measured wake paths in vertical and horizontal direction are given. It can be seen that all evaluated vortices follow the same trend. This can be assumed as the same condition was examined. Therefore, out of this measurements a mean line was derived, which gives the vertical and horizontal movement in this examination. It can be seen that the vortex stays in or near the rotor disk and does only feature a slight movement downwards until $\Psi = 50°$.

Afterwards a quite constant downward movement can be detected which is accelerated around $\Psi = 120°$. This effect may be introduced by the following blade. At higher wake ages it is more difficult to determine the vortex center. Furthermore, the scatter is becoming larger as also observed by Light[2]. This is due to the growing visibility problems of the fog visualized vortex cores.
It can be stated that, although the rotor is IGE, the mean horizontal movement is directing constantly inwards. The vortices A, D and F already show tendencies of a hampered contraction at high wake ages. The movement of the flow will later on reverse and finally point in outbound direction.

2.2 Numerical Examination

The numerical examination IGE is showing the same overall trend of an impingement flow, which is first contracting underneath the rotor and then deflected in outbound direction. In the inner region of the rotor a recirculating area can be found. Far away from the rotor the vortices are turning up. Figure 7 depicts

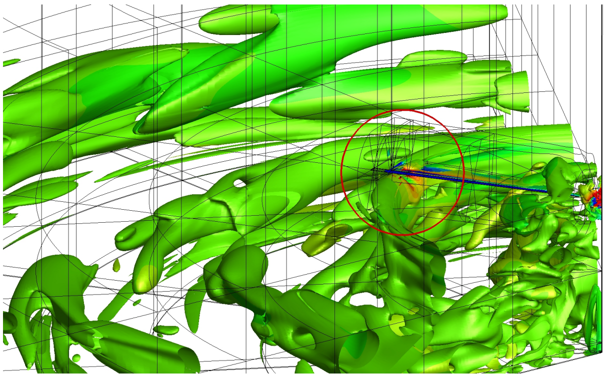

Fig. 7. Three-dimensional setup view featuring a λ_2 visualization of the vortices and pressure field contour

a three-dimensional view of the IGE setup. The vortices are visualized via the λ_2 criterion, whereas on the surface of the vortices the normalized pressure is shown. Especially around the blade a visible influence of the blade pressure field on the following vortex is found (see Fig. 7 red marked area), whereas the experimental results do not show such a considerable deflection, which should be found in the vertical movement around $\Psi = 120°$.
The high angle of attack, the low rotational velocity and the pile-up of the ground are leading to a flow instability in the inner section of the blade which results in a stalled inbound section, introducing even more disturbances to the inner flow field. Therefore, unsteady effects are assumed. The ground effect hampers the drain of these unsteady disturbances, so that these influences will last much longer and thus have a greater impact than OGE. Here (Fig. 8) the vortices are convected downwards with a constant inbound movement. The inbound section now features an attached flow, so nearly no unsteady effects are expected. Again the influence of the following blade on the previous vortex via the pressure field can be seen in the figure as the normalized pressure is depicted as contour.

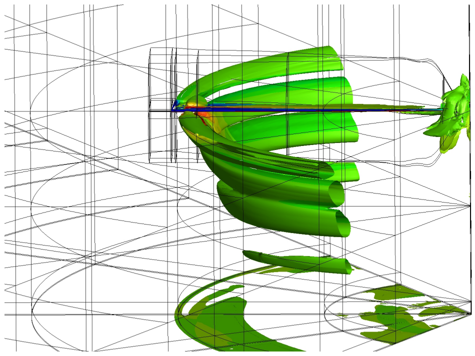

Fig. 8. Three-dimensional setup view OGE featuring a λ_2 visualization of the vortices and pressure field contour

2.2.1 Thrust value

As already mentioned the collective pitch IGE was modified until the thrust balanced the weight of the helicopter. A pitch angle of about $4°$ at the blade tip is necessary. At the end the mean thrust value was only about 0.4% lower than the experimental mean value (blue and green dotted lines in Fig. 9). According to all the simplifications and rounding of values, this is a perfectly trimmed result. As the mean value is trimmed no further conclusion can be drawn. Nevertheless the unsteady behavior of the thrust value is noteworthy especially as the helicopter is hovering in ground effect.
In Fig. 9 the mean thrust values (of one blade) are shown. Also the unsteady evolution of the CFD thrust is given. It is visible that the thrust features a non-negligible three per rev periodical oscillation around the mean value of about 10%. As this oscillation has a considerable effect a frequency analysis is also given in Fig. 9. There it can be detected that IGE disturbances are introduced over a wide spectrum, but the biggest influences are introduced with the blade passing frequency (BPF) and higher harmonics of the BPF. A similar observation was published in Ref. 13 for the forward flight of a model scale rotor. As those oscillations are of such a significant magnitude the location of the highest contribution to the oscillation in the thrust value are of interest. Therefore, Fig. 10 depicts the root mean square value of the oscillation in the thrust value over the last three revolutions over the

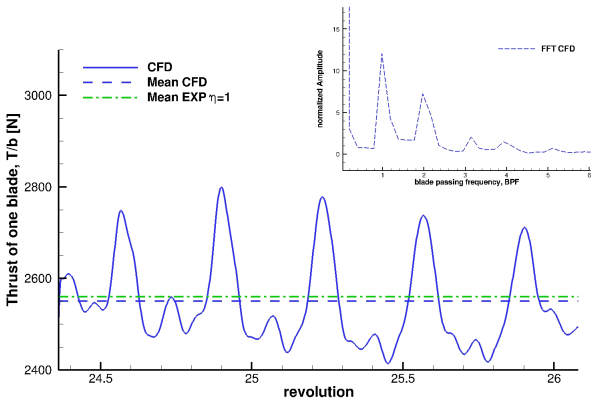

Fig. 9. Comparison of the thrust values and frequency analysis of the CFD thrust value

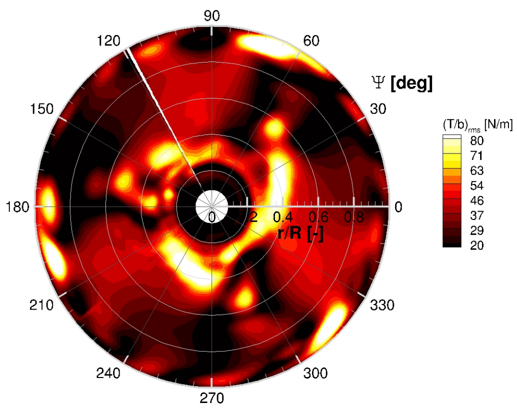

Fig. 10. Location analysis of the oscillation in thrust per blade

rotor disk. According to the previously found facts the main disturbances may be found triply on the revolution. Especially the influences at the outer rotor edge at $\Psi = 80, 200, 320°$ possess the main impact. The next biggest leverage on the oscillation are the disturbances at about $r/R = 0.2 - 0.6$ with a six per rev characteristics. Other minor impacts can be extracted, as found out in the frequency analysis, mainly at higher harmonics of the BPF like the twelve per rev oscillation at $r/R = 0.9$. The non harmonic impacts mainly result out of smearing effects between the harmonic disturbances. Oscillations with a spacial expansion over $120°$ and a time resolution above $1.4kHz$ (Nquist criterion leads to $2°$ of rotor revolution time resolution) are not resolved properly, as they exceed the spatial and time resolution of the solution. A reason for the disturbances in the thrust distribution may be reflexions at the ground surface which propagate back in the wake.
The OGE computation employs the collective pitch value previously found IGE to balance the weight. So conclusions can be drawn regarding the performance data. The blade was computed over six revolutions to assure a converged flow field. Two more revolutions were computed to average the thrust value. A much smoother development of the thrust is found OGE. Only negligible oscillations around the mean value are detected.
In Tab. 3 an overview of the achieved mean performance values is given. OGE the thrust at the same collective pitch setting is about 11% lower than IGE, whereas the moment for one blade M/b around the shaft axis and subsequently the power consumption of one blade P/b is nearly 4% higher OGE.
For a comparison the values are scaled according to the momentum theory with $P/b \sim M/b \sim (T/b)^{3/2}$. This leads to a benefit of 24% effectively due to the ground effect. At this h/R ratio this result fits well with the ground effect experiments in Ref. 2.

Table 3. Performance comparison IGE - OGE

$(T/b)_{IGE}$ [N]	$(T/b)_{OGE}$ [N]	Δ [%]
2550	2260	−11.4
M_{IGE} [Nm]	M_{OGE} [Nm]	Δ [%]
−560	−580	3.6

2.3 Comparison

To validate the flow solver for helicopter rotors in ground effect featuring correct scale, Reynolds numbers and Mach number a comparison between the computational results and the experiment is drawn.

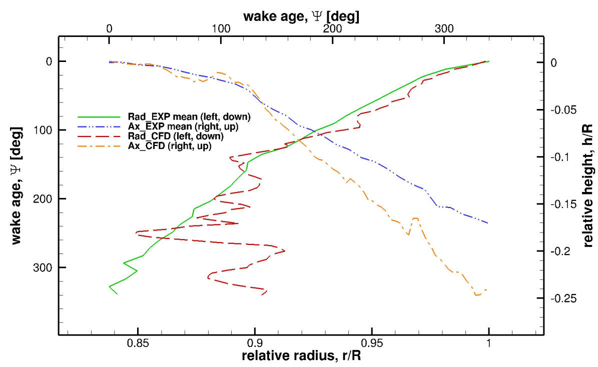

Fig. 11. Comparison of the wake paths of the experiment and the CFD calculation

In Fig. 11 the experimental and computational results of the wake paths are shown. The green (solid) and red (dashed) lines show the radial wake path comparison between the experiment and the computation (left ordinate and lower abscissa), whereas the blue (dash-dot-dotted) and orange (dash-dotted) lines represent the vertical evolution of the experimental and computational wake (right ordinate and upper abscissa).

It can be stated that the radial wake paths agree well until $\Psi = 240°$ when the unsteadiness in the CFD calculation strongly increases. This behavior indicates that also the mean value will feature a big scatter. Starting at that wake age, the computational wake stops contraction whereas the experimental mean path further contracts.

The computational axial path fits well the experimental one until a wake age of about $\Psi \approx 130°$. Afterwards the axial drain is overestimated compared to the experiment. This behavior was also found in previous validation runs e.g. Ref. 13. As observed in Fig. 7 around $\Psi = 120°$ a deflection in the wake path is observed. The reason for the absence of that characteristic in the experiment may be due to the low resolution of the experimental flow field. Especially the vortices E and F (Figs. 5-6) show tendencies of a blade influence on the wake path. Therefore, the numerical finding is also present in the experimental examination.

3 SUMMARY

A Hughes 300C hovering IGE was examined experimentally to obtain the movement of the blade vortices. A study to analyze the characteristics of the wake was performed. Quantized data were also collected along the wake trajectory. The vortices could be detected and visualized in the first $360°$ of wake age. Longer tracking of the vortices was not possible due to the instable characteristics of the visualized vortices at high wake ages and the limited resolution capability of the high performance camera. Nevertheless, important data could be achieved which serve for CFD code validation purposes.

In a next step a computational one-third model with periodic and ground boundaries was built up and examined with the unsteady RANS flow solver FLOWer. The thrust was trimmed to the weight of the system and the blade dynamics were neglected. Overall a good reproduction of the wake path was obtained with a slight overestimation of the axial wake path. The unsteady effects in the ground proximity are leading to a considerable oscillation in the thrust value over time. Especially at higher harmonics of the BPF disturbances are found.

In the last step the ground wall was removed to compute an OGE setup. The same collective setting was employed. The vortices convect downwards and inwards as expected, also a smooth development of the thrust value was found with nearly no oscillations and unsteady effects. The analysis of the performance data leads to an 24% benefit due to the ground effect. Further analysis to evaluate the influence of the blade dynamics on the thrust value development in ground effect and a higher order approach to realize a better conservation of the wake and, therefore, all its unsteady effects, as well as the examination of the fuselage impact on the fluid motion will be the next steps.

ACKNOWLEDGMENTS

In memoriam Tobias Großmann.

REFERENCES

[1] Landgrebe, A. J., “The wake geometry of a hovering helicopter rotor and its influence on rotor performance,” Proceedings of the American Helicopter Society, 28th Annual Forum, May 1972.

[2] Light, J. S., “Tip vortex geometry of a hovering helicopter rotor in ground effect,” Proceedings of the American Helicopter Society, 45th Annual Forum, Boston, MA, 1989.

[3] Curtiss, H. C., Sun, M., Putman, W. F., and Hanker Jr., W. J., “Rotor aerodynamics in ground effect at low advance ratios,” Proceedings of the American Helicopter Society, 37th Annual Forum, New Orleans, LA, May 1981.

[4] Nathan, N. D. and Green, R. B., “The flow around a model helicopter main rotor in ground effect,” *Experiments in Fluids*, Vol. 52, 2012, pp. 151–166.

[5] Hayden, J. S., “The effect of the ground on helicopter hovering power required,” Proceedings of the American Helicopter Society, 32nd Annual Forum, Washington, D.C., 1976.

[6] Xin, H., Prasad, J., and Peters, D. A., “An analysis of partial ground effect on the aerodynamics of a helicopter rotor,” AIAA 38th Aerospace Sciences Meeting and Exhibit, Reno, NV, January 2000.

[7] Bhattacharyya, S. and Conlisk, A., “The structure of the rotor wake in ground effect,” AIAA 41th Aerospace Sciences Meeting and Exhibit, Reno, NV, January 2003.

[8] D’Andrea, A., “Unsteady numerical simulations of helicopters and tiltrotors operating in sandy-desert environment,” Proceedings of the American Helicopter Society Specialist’s Conference on Aeromechanics, San Francisco, CA, January 2010.

[9] Brown, R. E. and Whitehouse, G. R., “Modelling rotor wakes in ground effect,” *Journal of the American Helicopter Society*, Vol. 49, (3), 2004, pp. 238–249.

[10] Kalra, T. S., Lakshminarayan, V. K., and Baeder, J. D., “CFD validation of micro hovering rotor in ground effect,” Proceedings of the American Helicopter Society, 66th Annual Forum, Phoenix, AZ, May 2010.

[11] Schmid, S., Lutz, T., and Krämer, E., “Impact of ground modelling approaches on the prediction of ground effect aerodynamics,” *Engineering Applications of Computational Fluid Mechanics*, Vol. 3, (3), 2009, pp. 419–429.

[12] Kutz, B. M., Bensing, F., Kessler, M., and Krämer, E., “CFD calculation of a helicopter rotor hovering in ground effect,” STAB Meeting, Berlin, Germany, November 2010.

[13] Kutz, B. M., Kowarsch, U., Kessler, M., and Krämer, E., “Numerical investigation of helicopter rotors in ground effect,” Paper AIAA-2012-2913, 30th AIAA Applied Aerodynamics Conference, New Orleans, La., 2012.

[14] Kroll, N., Eisfeld, B., and Bleeke, H., “The Navier-Stokes code FLOWer,” *Notes on Numerical Fluid Mechanics*, 1999, pp. 58–71.

[15] Jameson, A., Schmidt, W., and Turkel, E., “Numerical solutions of the Euler equations by finite volume methods using Runge-Kutta time-stepping schemes,” AIAA 14th Fluid and Plasma Dynamic Conference, Palo Alto, CA, 1981.

[16] Jameson, A., “Time dependent calculations using multigrid, with applications to unsteady flows past airfoils and wings,” AIAA 10th Computational Fluid Dynamics Conference, Honolulu, HI, 1991.